Relationship of cloud flare ups, growth of divergence, enhancement of the departures from balance laws and hurricane intensity

T. N. Krishnamurti

HSRP Science Team Meeting, FSU, Tallahassee, April 6-8 2009

Collaborators: Anu Simon, Mrinal Biswas, Christopher Davis

ARW Model Description

The real-time ARW forecasts in 2005 used a two-way nested configuration (Michalakes et al. 2005), that featured a 12-km outer fixed domain with a movable nest of 4/1.33-km grid spacing.

The nest was centered on the location of the minimum 500-hPa geopotential height within a prescribed search radius from the previous position of the vortex center (or within a radius of the first guess, when first starting).

Nest repositioning was calculated every 15 simulation minutes and the width of the search radius was based on the maximum distance the vortex could move at 40 m s^{-1}.

On the 12-km domain, the Kain–Fritsch cumulus parameterization was used, but domains with finer resolution had no parameterization.

All domains used the WRF single-moment 3-class (WSM3) microphysics scheme (Hong et al. 2004) that predicted only one cloud variable (water for $T > 0°C$ and ice for $T < 0°C$) and one hydrometeor variable, either rainwater or snow (again thresholded on 0°C).

Both domains also used the Yonsei University (YSU) scheme for the planetary boundary layer (Noh et al. 2003).

This is a first-order closure scheme that is similar in concept to the scheme of Hong and Pan (1996), but appears less biased toward excessive vertical mixing as reported by Braun and Tao (2000).

The drag formulation follows Charnock (1955) and is described more in section 5. The surface exchange coefficient for water vapor follows Carlson and Boland (1978), and the heat flux uses a similarity relationship (Skamarock et al. 2005).

The forecasts were integrated from 0000 UTC and occasionally 1200 UTC during the time when a hurricane threatened landfall within 72 h.

Forecasts were initialized using the Geophysical Fluid Dynamics Laboratory (GFDL) model, with data on a ⅙° latitude–longitude grid. The Global Forecast Model (GFS) from the National Centers for Environmental Prediction (NCEP), obtained on a 1° grid, was used only when the GFDL was unavailable.

Davis, C., W. Wang, S.S. Chen, Y. Chen, K. Corbosiero, M. DeMaria, J. Dudhia, G. Holland, J. Klemp, J. Michalakes, H. Reeves, R. Rotunno, C. Snyder, and Q. Xiao, 2008: Prediction of Landfalling Hurricanes with the Advanced Hurricane WRF Model. *Mon. Wea. Rev.*, 136, 1990–2005.

Post processing diagnostics

Here we shall be showing some post processing for WRF-ARW. This model is presently being added to our suite of mesoscale models.

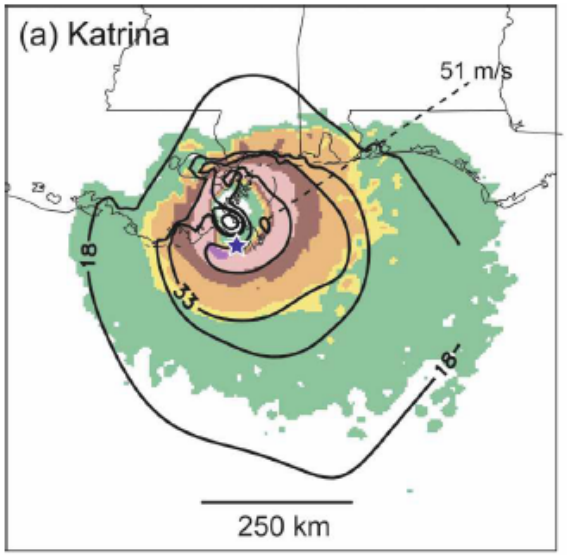

Katrina, valid time = 1200 UTC 29 Aug (60-h forecast)

10-m wind from AHW real-time forecasts with contours of nearest HWind (black lines) analyses overlaid

Predicted storm center location at indicated valid times (below) is denoted by blue star in each figure. Wind fields from AHW forecasts have been shifted to observed locations to facilitate comparison.

HWind valid times are (a) 1132 UTC 29 Aug

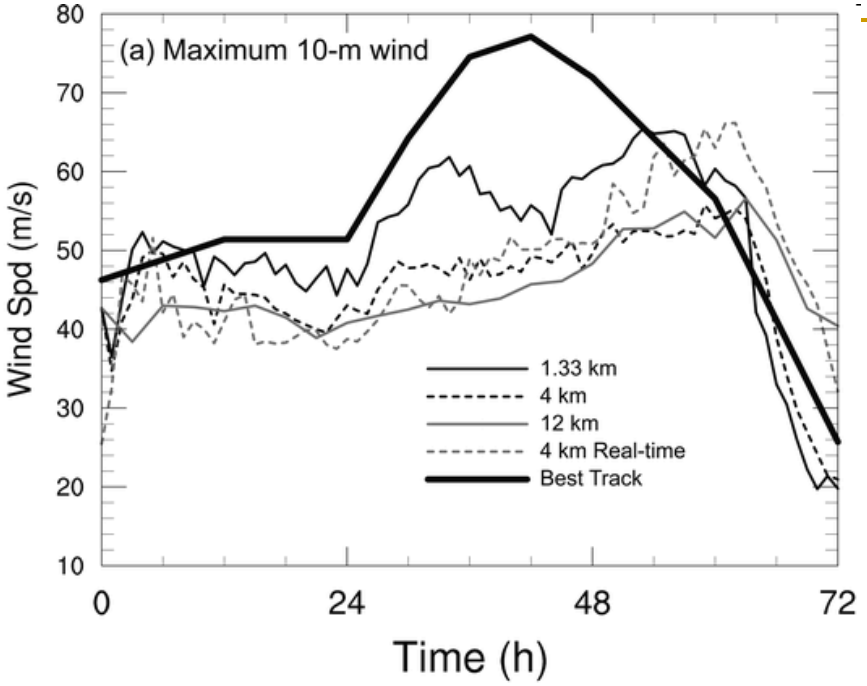

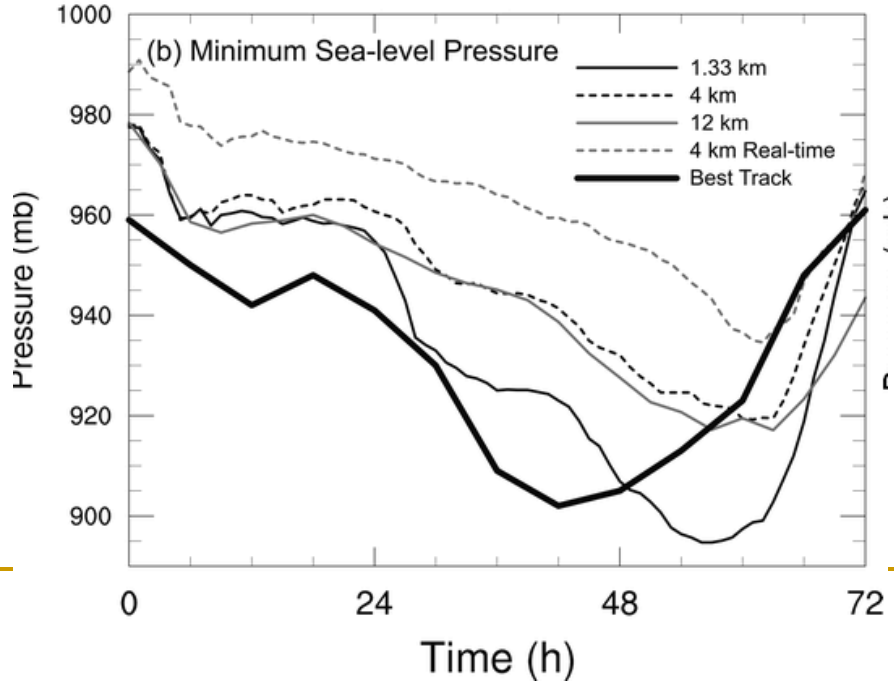

Predicted intensity and minimum sea level pressure at different forecast hours

(a) Maximum 10-m wind and (b) minimum sea level pressure for forecasts of Katrina beginning 0000 UTC 27 Aug. Legend labels 1.33, 4, and 12 km refer to grid spacing of WRF ARW, version 2.1.2, using the Charnock drag relation. The forecast on a 12-km grid used the Kain–Fritsch parameterization. The 4-km real time (gray dashed) refers to the forecast made in real time with an innermost nest of 4-km grid spacing. All retrospective forecasts were initialized with the GFDL initial condition.

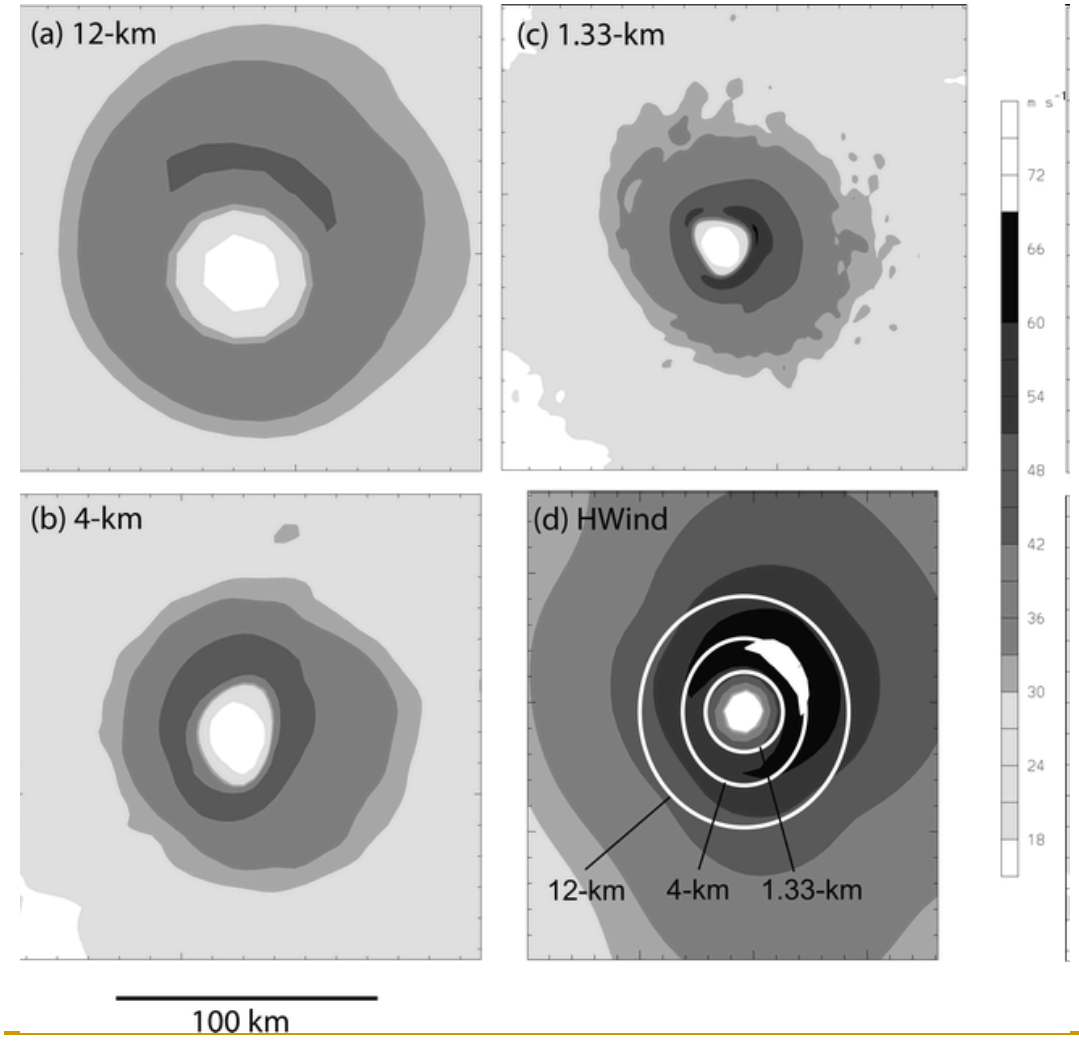

Size of the storm as seen by the predicted wind field at different resolutions compared to HWIND.

Shown here is 10-m wind speed (m s−1) from 36-h Katrina forecast valid 1200 UTC 28 Aug on (a) the 12-km grid, (b) the 4-km grid, (c) the 1.33-km grid, and (d) the NOAA HWind product valid 1200 UTC 28 Aug. White ellipses in (d) are an approximate trace of the radii of maximum wind at each azimuth around the vortices in (a), (b), and (c).

1.33 km

4 km

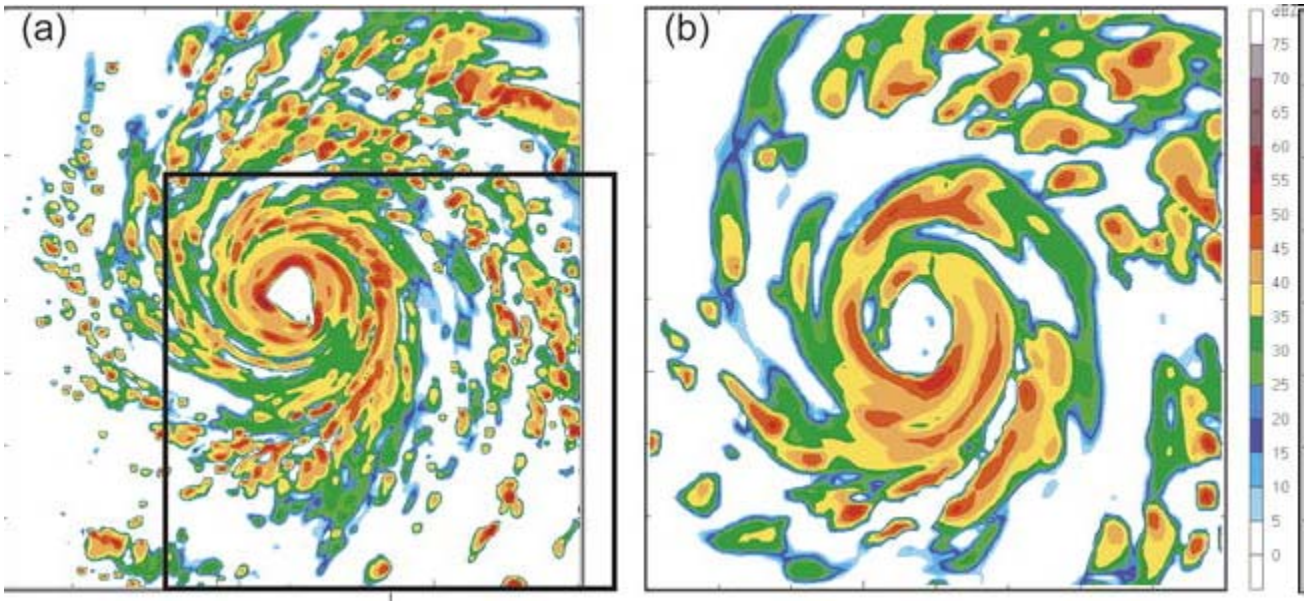

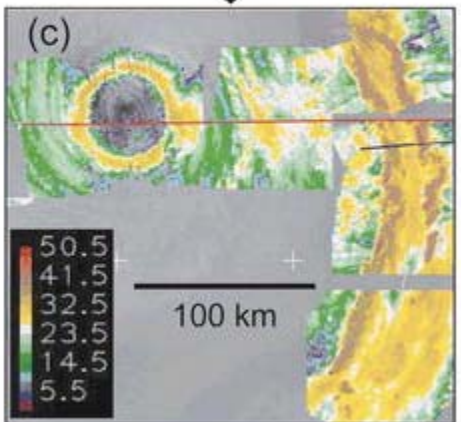

OBS composite radar

Model-derived reflectivity at 3-km MSL valid 2300 UTC 28 Aug from nest with (a) 1.33-km grid increment and (b) 4-km grid increment. (c) Observed radar reflectivity composite valid between 2000 and 2100 UTC 28 Aug based on tail Doppler radar data from both the NOAA P-3 (red track) and the Naval Research Laboratory P-3 (pink track) with the Electra Doppler radar (ELDORA). The composite radar image was obtained from the RAINEX field catalog maintained by the Earth Observing Laboratory of the National Center for Atmospheric Research.

We shall next illustrate several examples of the following scenario:

1. **Deep convection flares up near the eye wall, as seen from the local growth of rain water mixing ratio, liquid water mixing ratio or radar reflectivity as implied from model hydrometeors.**
2. **Divergence flares up**
3. **Departures from balance laws flare up**
4. **Solution of complete radial equation shows rapid growth of hurricane intensity.**

Departures from balance laws

The full divergence equation can be written in the form (from Fankhauser 1974):

$$-\nabla^2\phi = -f\left(\frac{\partial u}{\partial y} - \frac{\partial v}{\partial x}\right) - 2\left(\frac{\partial v}{\partial x}\frac{\partial u}{\partial y} - \frac{\partial u}{\partial x}\frac{\partial v}{\partial y}\right) + \beta u + \left(\frac{\partial \omega}{\partial x}\frac{\partial u}{\partial p} + \frac{\partial \omega}{\partial y}\frac{\partial v}{\partial p}\right) + D^2 +$$

$$\left(\frac{\partial D}{\partial t} + u\frac{\partial D}{\partial x} + v\frac{\partial D}{\partial y} + \omega\frac{\partial D}{\partial p}\right) + \left(\frac{\partial F_u}{\partial x} + \frac{\partial F_v}{\partial y}\right)$$

Red lines represent the balance equation (Haltiner and Williams 1980). The blue underlined terms denote the non linear balance which is also expressed as .

$$\nabla^2\phi = f\nabla^2\psi + 2J\left(\frac{\partial \psi}{\partial x}, \frac{\partial \psi}{\partial y}\right)$$

Implication of gradient wind departures on hurricane intensity

In local cyclindrical storm centered coordinate we can write the complete radical equation of motion in the form:

$$\frac{\partial V_r}{\partial t}+V_\theta\frac{\partial V_r}{r\partial\theta}+V_r\frac{\partial V_r}{\partial r}+\omega\frac{\partial V_r}{\partial p}-\frac{V_\theta^2}{r}-fV_\theta=-g\frac{\partial z}{\partial r}+F_r \text{ or}$$

$$\frac{V_\theta^2}{r}+fV_\theta-g\frac{\partial z}{\partial r}+GWD=0 \text{ where GWD denotes the gradient wind departure.}$$

Where $GWD=-\frac{\partial V_r}{\partial t}-V_\theta\frac{\partial V_r}{r\partial\theta}-V_r\frac{\partial V_r}{\partial r}-\omega\frac{\partial V_r}{\partial p}-F_r$

V_θ can be expressed by the relation, $V_\theta=\dfrac{-f\pm\sqrt{f^2-\frac{4}{r}\left(GWD-g\frac{\partial z}{\partial r}\right)}}{\frac{2}{r}}$.

This denotes a local value of the tangential wind from a complete radial wind equation in the presence of gradient wind departures GWD. Note that $-g\frac{\partial z}{\partial r}$ is generally <0 in the inner rain area (r<200 km where r is positive outward). The gradient wind, in this locale storm centered coordinate, is given by: $V_{\theta_g}=\dfrac{-f\pm\sqrt{f^2+\frac{4}{r}\left(g\frac{\partial z}{\partial r}\right)}}{\frac{2}{r}}$. Note that GWD can be $\leqslant 0$. Thus several possibilities exist:

If $f^2<\frac{4}{r}\left(GWD-g\frac{\partial z}{\partial r}\right)$ we have a nonphysical solution.

We are looking for different options for $f^2 - \frac{4}{r}\left(GWD - g\frac{\partial z}{\partial r}\right) \rangle 0$, and its positive root.

Since $g\frac{\partial z}{\partial r} \rangle 0$ we can write the inequality in the form, $f^2 + \frac{4}{r}g\frac{\partial z}{\partial r} \rangle \frac{4}{r}GWD$. The left hand side is essentially positive definite, GWD<0 would always satisfy this condition. A negative value of GWD contributes to a value of V_θ in equation () larger than the gradient wind value, i.e. $V_\theta \rangle V_{\theta g}$, hence the extreme negative values of GWD would go with large values of azimuthal motions i.e. supergradient winds or non physical situations. A positive value of GWD, conversely describes situations with subgradient winds. Such instances of very strong azimuthal motions described by the complete radial equation of motion, are attributed to the departure from gradient wind (GWD) which also relate to large values of divergence, this we illustrate below.

A note on Radial gradient wind solution:

For a hurricane in storm centered coordinate the radial gradient wind equation is expressed by $\frac{V_\theta^{\,2}}{r} + fV_\theta = g\frac{\partial z}{\partial r}$ where $\frac{V_\theta^{\,2}}{r}$, fV_θ and $g\frac{\partial z}{\partial r}$ are all generally positive. The roots of this equation are $u = \frac{-f \pm \sqrt{\frac{4}{r}g\frac{\partial z}{\partial r}}}{\frac{2}{r}}$. Note that the negative root of the radical is nonphysical hence there is only one positive root i.e. $\frac{-f + \sqrt{\frac{4}{r}g\frac{\partial z}{\partial r}}}{\frac{2}{r}}$ for $\left|\sqrt{\frac{4}{r}g\frac{\partial z}{\partial r}}\right| \rangle |f|$.

This implies that $\sqrt{\frac{4}{r}g\frac{\partial z}{\partial r}} \rangle f$ applies for cyclonic motions. Note that there are no anomalous solutions of the radical gradient wind equation, i.e. there is only one normal

solution. Such instances of very strong azimuthal motions, described by the complete radical equation of motion, are attributed to the departures from gradient wind (GWD) which relate to large values of divergence.

The full divergence equation can be written in the form (from Fankhauser 1974):

$$-\nabla^2\phi = -f\left(\frac{\partial V_\theta}{\partial y} - \frac{\partial V_r}{\partial x}\right) - 2\left(\frac{\partial V_r}{\partial x}\frac{\partial V_\theta}{\partial y} - \frac{\partial V_\theta}{\partial x}\frac{\partial V_r}{\partial y}\right) + \beta u + \left(\frac{\partial \omega}{\partial x}\frac{\partial V_\theta}{\partial p} + \frac{\partial \omega}{\partial y}\frac{\partial V_r}{\partial p}\right) + D^2 +$$

$$\left(\frac{\partial D}{\partial t} + V_\theta\frac{\partial D}{\partial x} + V_r\frac{\partial D}{\partial y} + \omega\frac{\partial D}{\partial p}\right) + \left(\frac{\partial F_{V_\theta}}{\partial x} + \frac{\partial F_{V_r}}{\partial y}\right)$$

Red lines represent the balance equation (Haltiner and Williams 1980). The underlined terms denote the non linear balance which is also expressed as $\nabla^2\phi = f\nabla^2\psi + 2J\left(\frac{\partial\psi}{\partial x}, \frac{\partial\psi}{\partial y}\right)$.

The complete radial equation of motion in storm centered coordinate (r positive outward) is written in the form:

$$\frac{dV_r}{dt} - \underline{\left(f + \frac{V_\theta}{r}\right)V_\theta = -\frac{\partial\phi}{\partial r}} + g\frac{\partial\tau_\theta}{\partial p}$$

Or $\frac{\partial V_r}{\partial t} = -V_\theta\frac{\partial V}{r\partial\theta} - V_r\frac{\partial V_r}{\partial r} - \omega\frac{\partial V_r}{\partial p} - \underline{\frac{V_\theta^2}{r} - fV_\theta = -g\frac{\partial z}{\partial r}} + F_r$, the underlined terms denote radial gradient wind balance. The non linear balance and the radial gradient wind equation are equivalent, Fortak (1956).

Fortak, H., "Concerning the general vertically averaged hydrodynamic equations NHRP report no. 51, U.S. Weather Bureau, Washington, DC, Apr. 1962.

Thus departures from non linear balance can be approximately equated to departures from gradient wind balance for the radial direction. Departures from non linear balance largely arise from horizontal and vertical advection of divergence and the divergence square. If a flare up of deep convection occurs near the eye wall of a hurricane divergence (/convergence) increases, so do the departures from balance laws. Growth of negative departures leads to a stronger hurricane. This follows from

$$GWD' = \left(\frac{\partial \omega}{\partial x}\frac{\partial u}{\partial p} + \frac{\partial \omega}{\partial y}\frac{\partial v}{\partial p}\right) + D^2 + \left(\frac{\partial D}{\partial t} + u\frac{\partial D}{\partial x} + v\frac{\partial D}{\partial y} + \omega\frac{\partial D}{\partial p}\right) + \left(\frac{\partial F_u}{\partial x} + \frac{\partial F_v}{\partial y}\right)$$

The complete radial equation may be written as where "GWD" denotes gradient wind departures, and GWD is expressed by the radial wind equations carries the solutions

$$\frac{V_\theta^2}{r} + fV_\theta - g\frac{\partial z}{\partial r} + GWD' = 0$$

the negative root is non physical. The other root, when GWD$'$ is $<<0$, carries strong tangential wind for its solution. When GWD$'=0$ then we have a radial gradient wind balance.

$$\frac{V_\theta^2}{r} + fV_\theta = g\frac{\partial z}{\partial r}$$

We have routinely mapped the field of GWD$'$ in the intensifying and decaying phases of hurricane intensity.

We have routinely mapped the field of GWD/ in the intensifying and decaying phases of hurricane intensity.

We shall next illustrate several examples of the following scenario:

1. **Deep convection flares up near the eye wall, as seen from the local growth of rain water mixing ratio, liquid water mixing ratio or radar reflectivity as implied from model hydrometeors.**
2. **Divergence flares up**
3. **Departures from balance laws flare up**
4. **Solution of complete radial equation shows rapid growth of hurricane intensity.**

Hourly plots

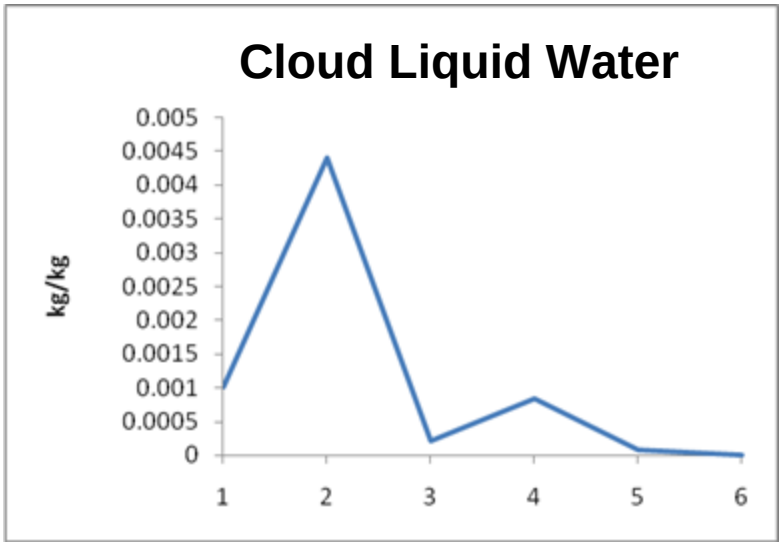

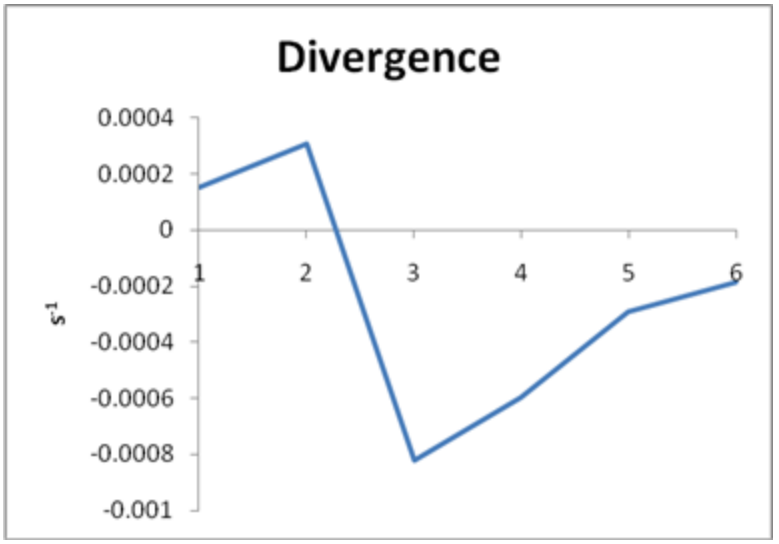

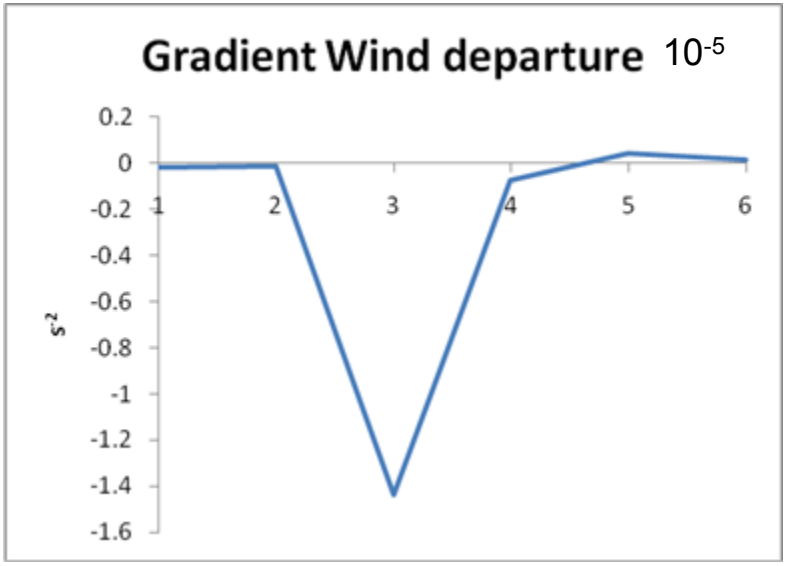

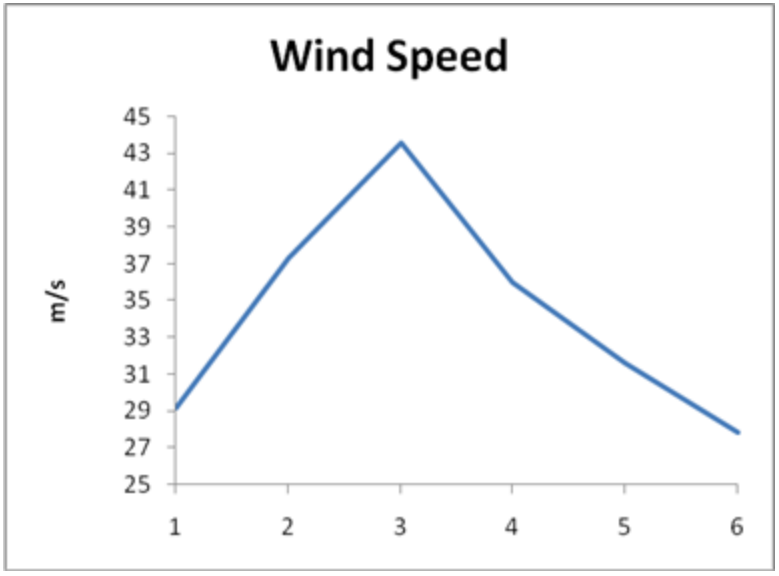

Initial time: 10z 28 August 2005

Hourly plots

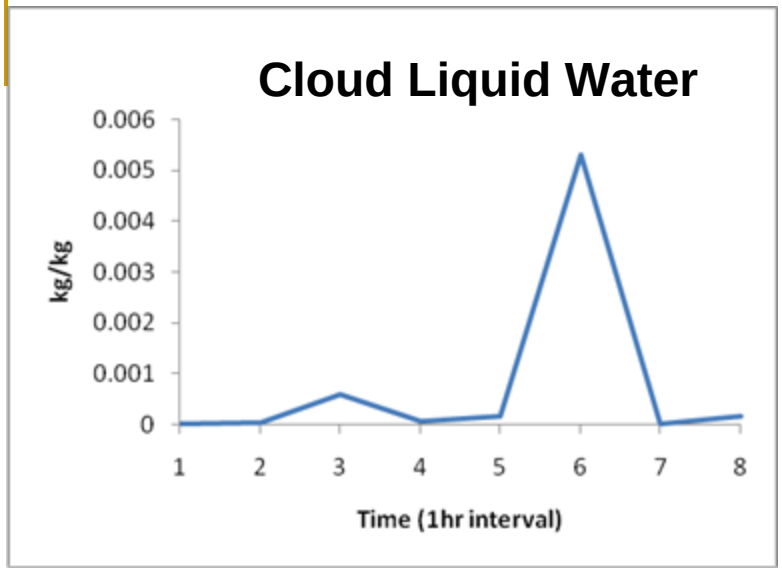

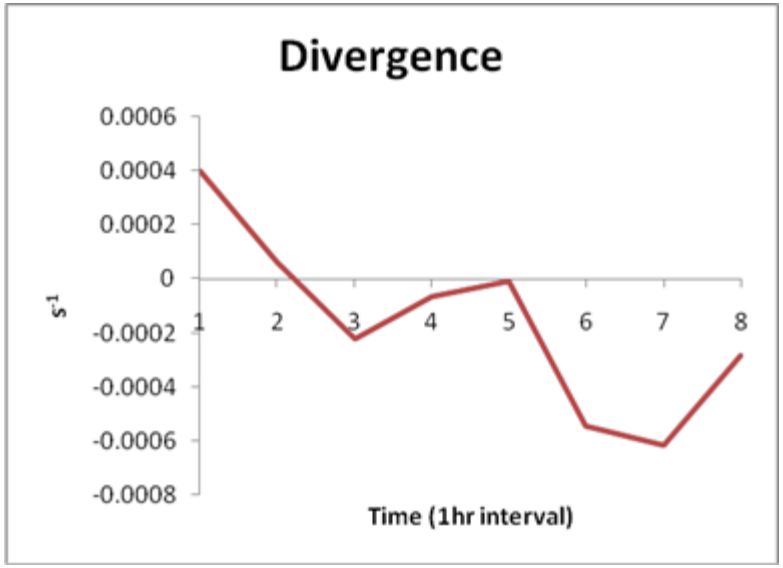

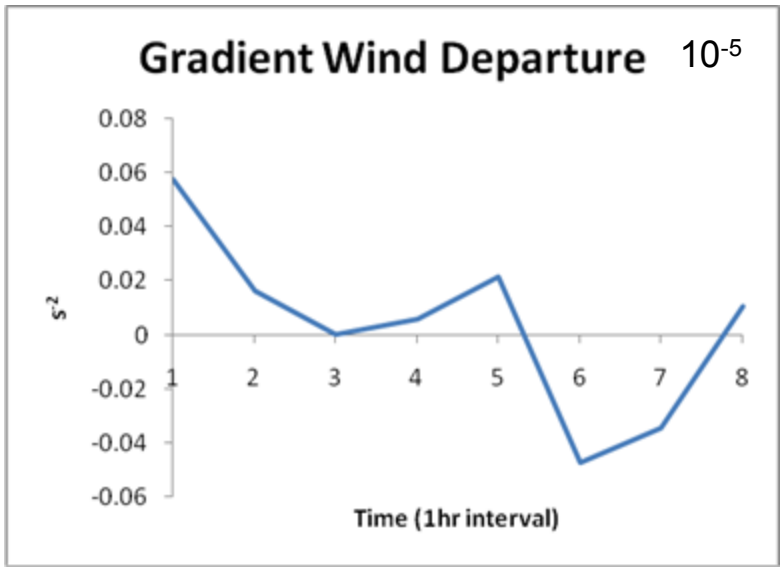

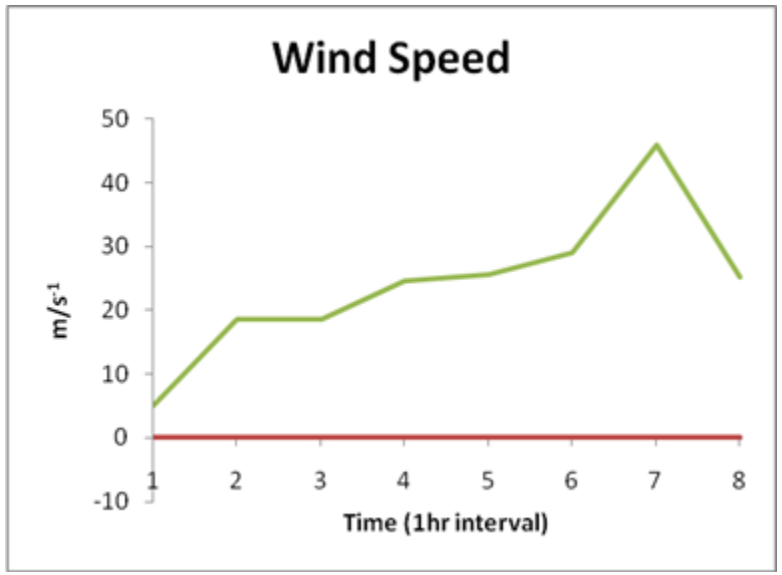

Initial time: 09z 28 August 2005

Hourly plots

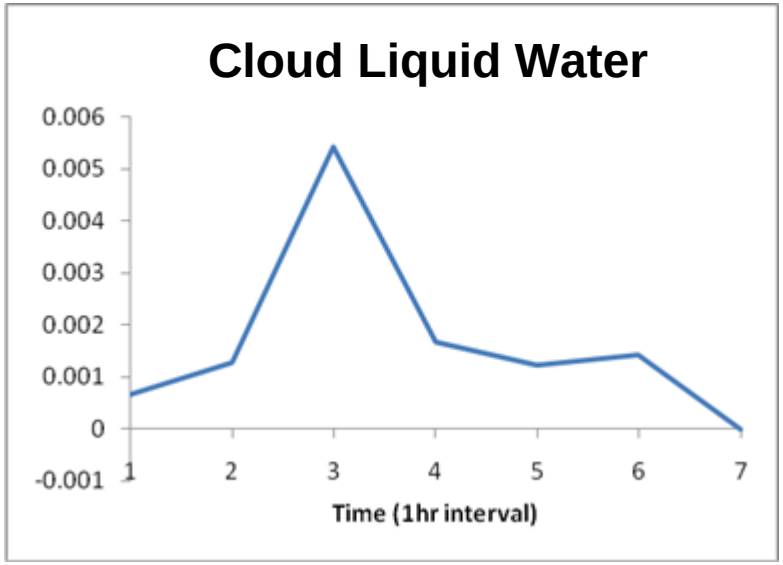

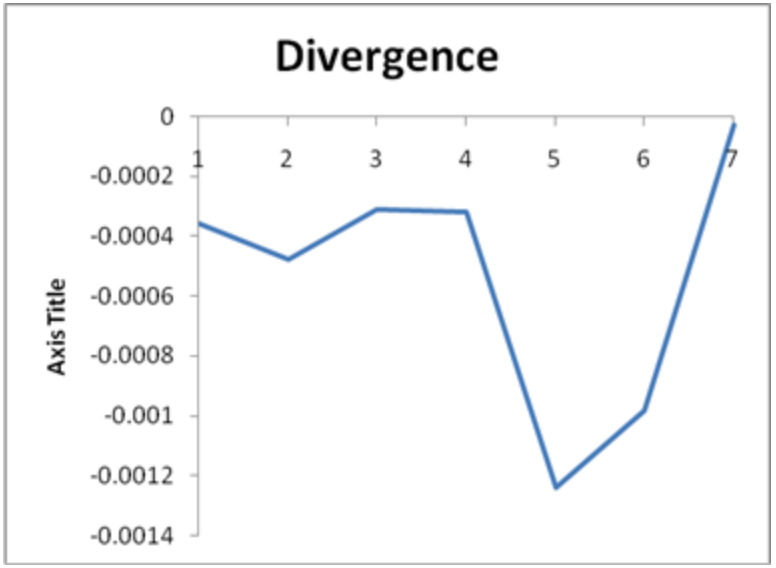

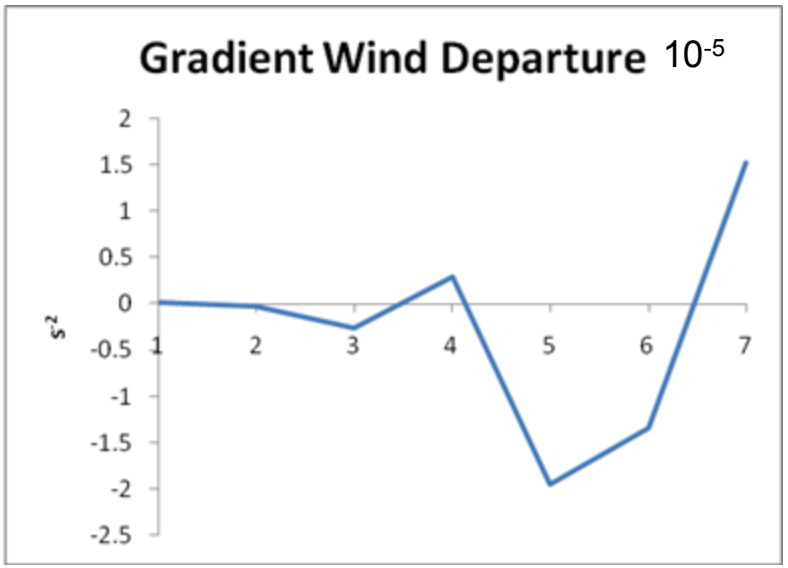

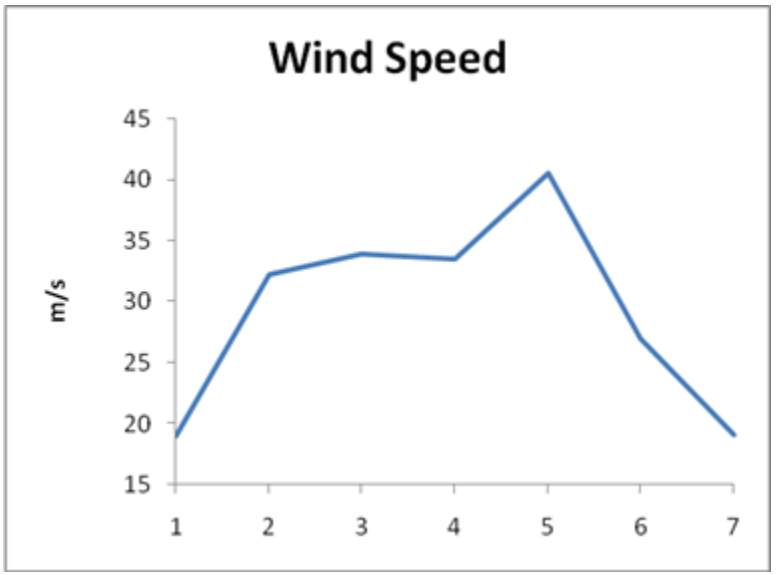

Initial time: 09z 28 August 2005

Hourly plots

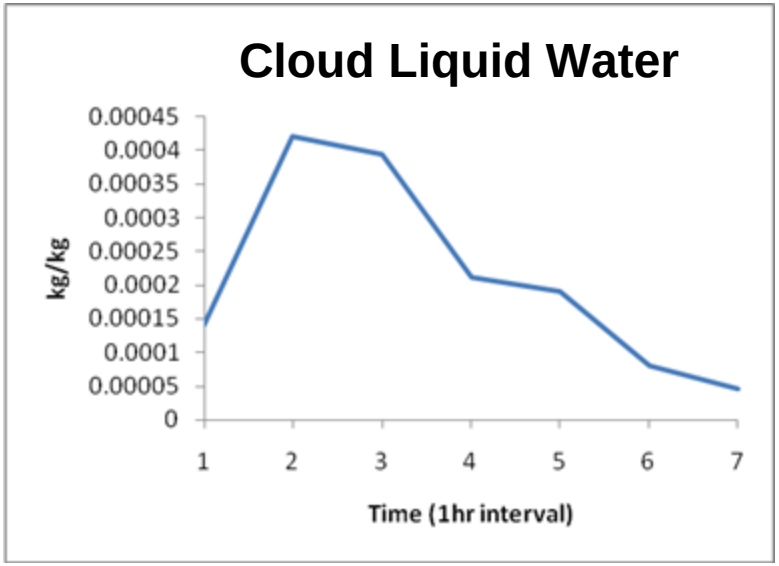

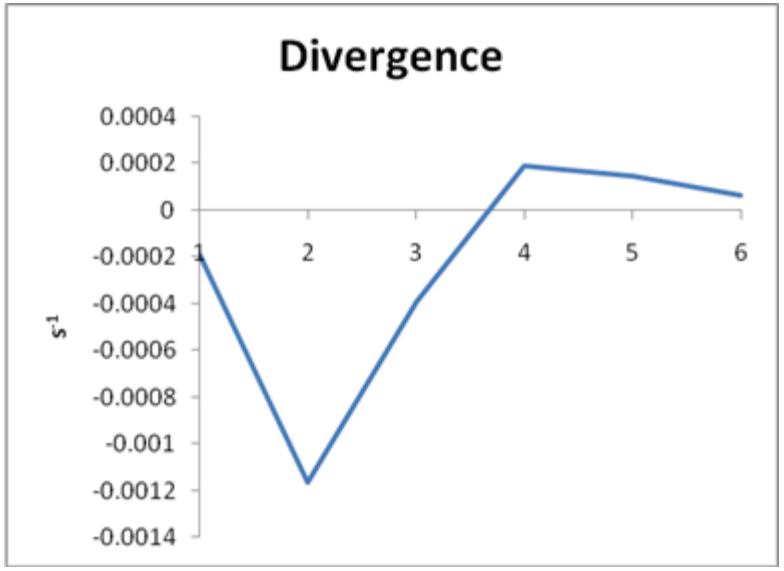

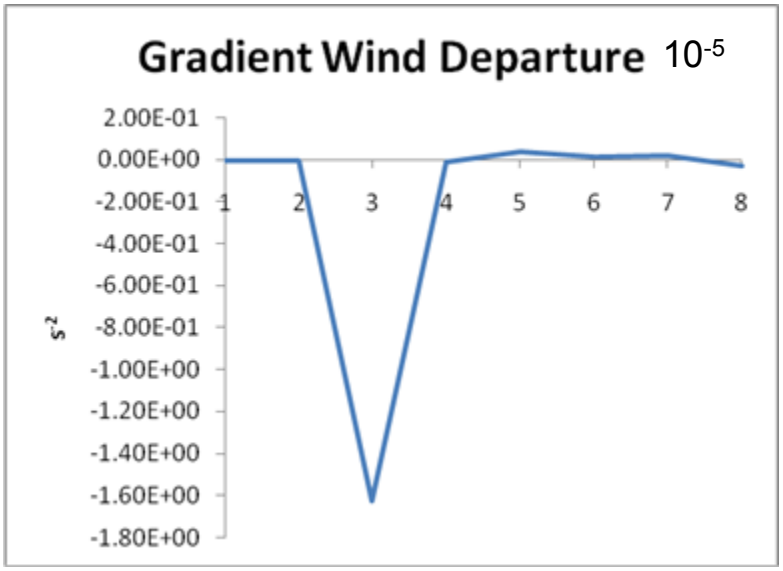

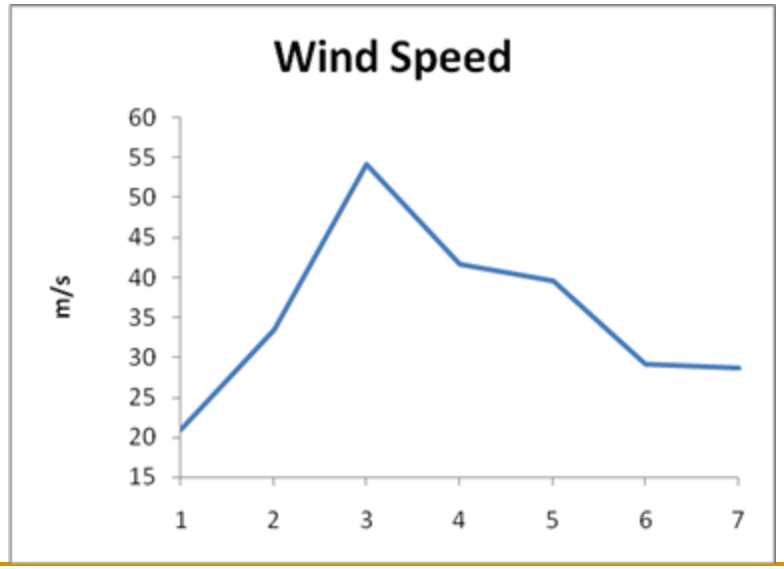

Initial time: 09z 28 August 2005

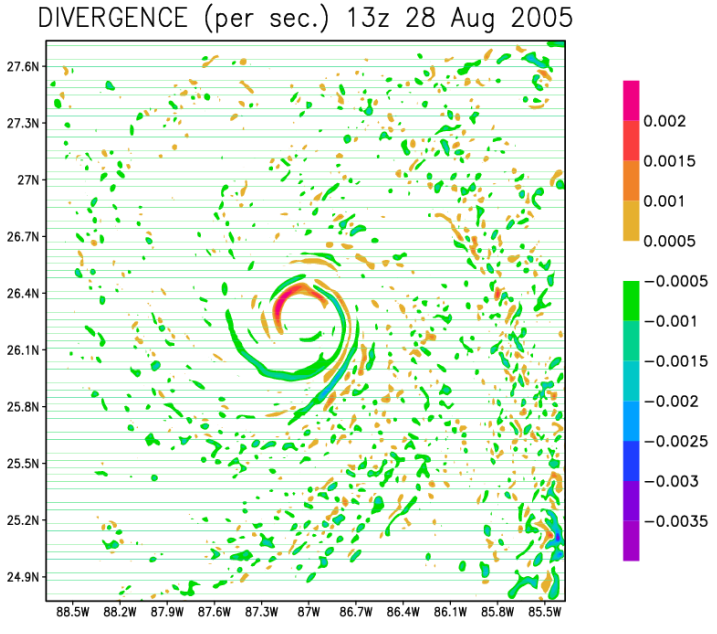
DIVERGENCE (per sec.) 13z 28 Aug 2005
27.6N
27.3N
27N
26.7N
26.4N
26.1N
25.8N
25.5N
25.2N
24.9N
88.5W 88.2W 87.9W 87.6W 87.3W 87W 86.7W 86.4W 86.1W 85.8W 85.5W
0.002
0.0015
0.001
0.0005
−0.0005
−0.001
−0.0015
−0.002
−0.0025
−0.003
−0.0035

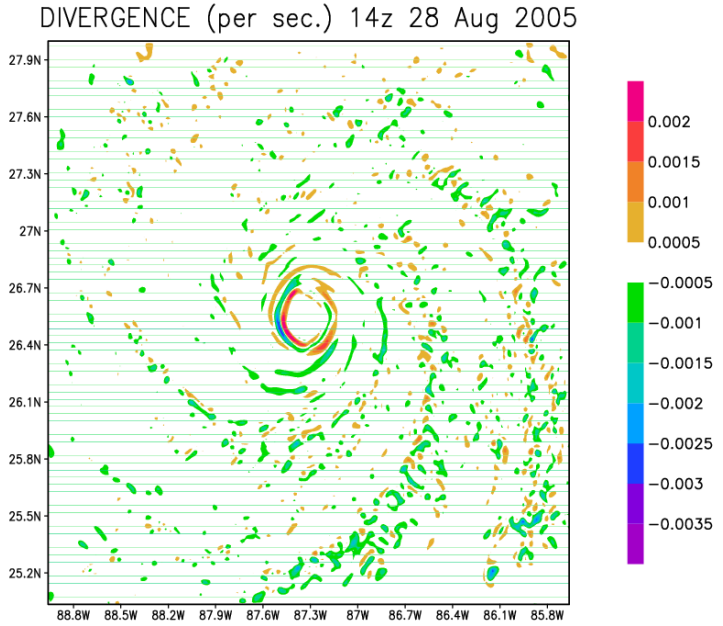
DIVERGENCE (per sec.) 14z 28 Aug 2005
27.9N
27.6N
27.3N
27N
26.7N
26.4N
26.1N
25.8N
25.5N
25.2N
88.8W 88.5W 88.2W 87.9W 87.6W 87.3W 87W 86.7W 86.4W 86.1W 85.8W
0.002
0.0015
0.001
0.0005
−0.0005
−0.001
−0.0015
−0.002
−0.0025
−0.003
−0.0035

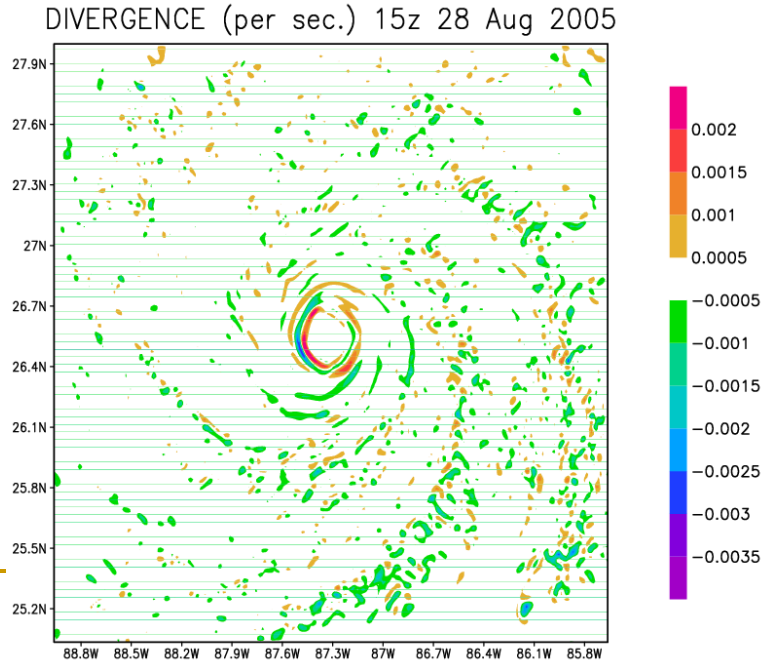
DIVERGENCE (per sec.) 15z 28 Aug 2005
27.9N
27.6N
27.3N
27N
26.7N
26.4N
26.1N
25.8N
25.5N
25.2N
88.8W 88.5W 88.2W 87.9W 87.6W 87.3W 87W 86.7W 86.4W 86.1W 85.8W
0.002
0.0015
0.001
0.0005
−0.0005
−0.001
−0.0015
−0.002
−0.0025
−0.003
−0.0035

DIVERGENCE

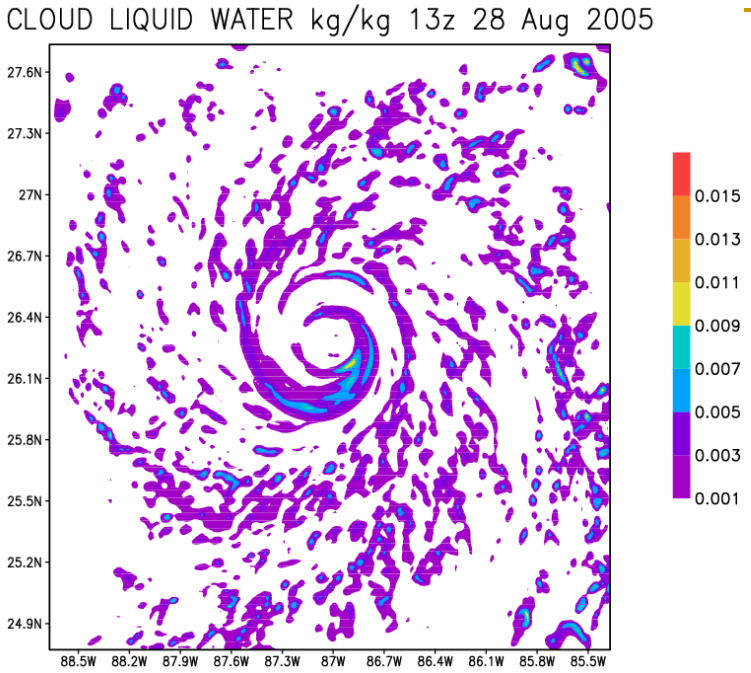

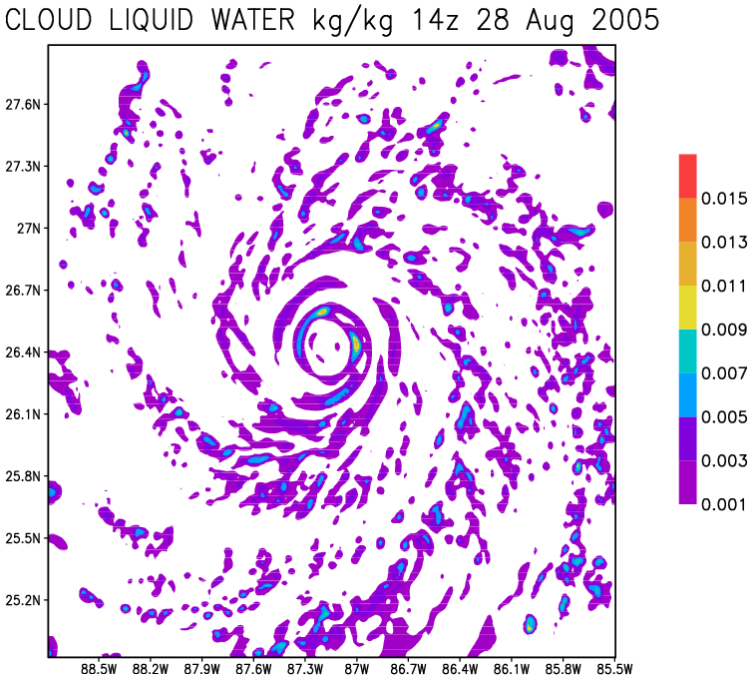

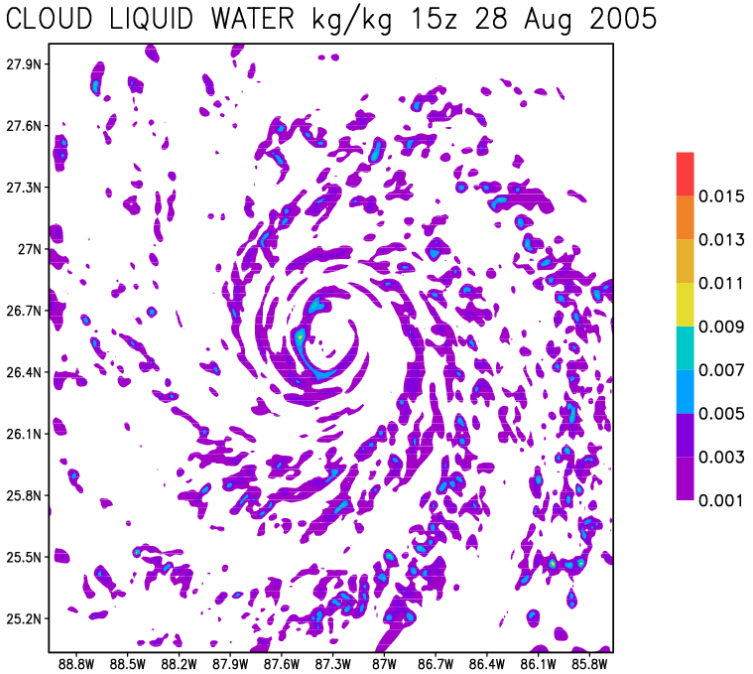

CLOUD LIQUID WATER

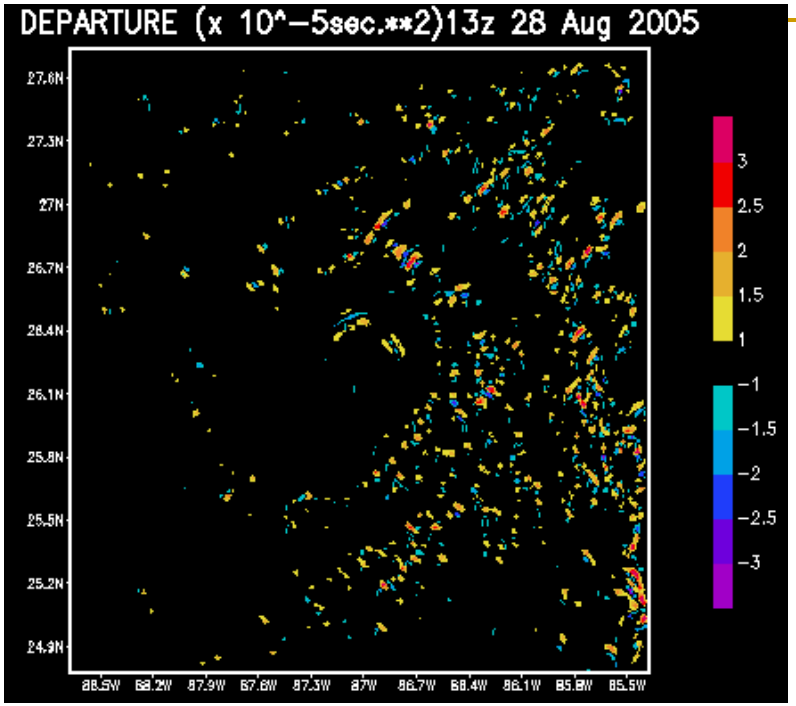

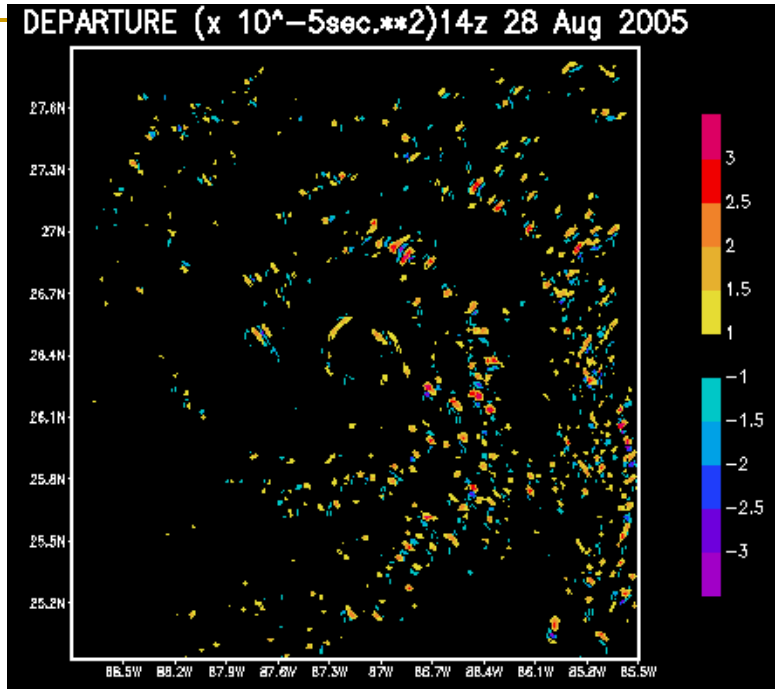

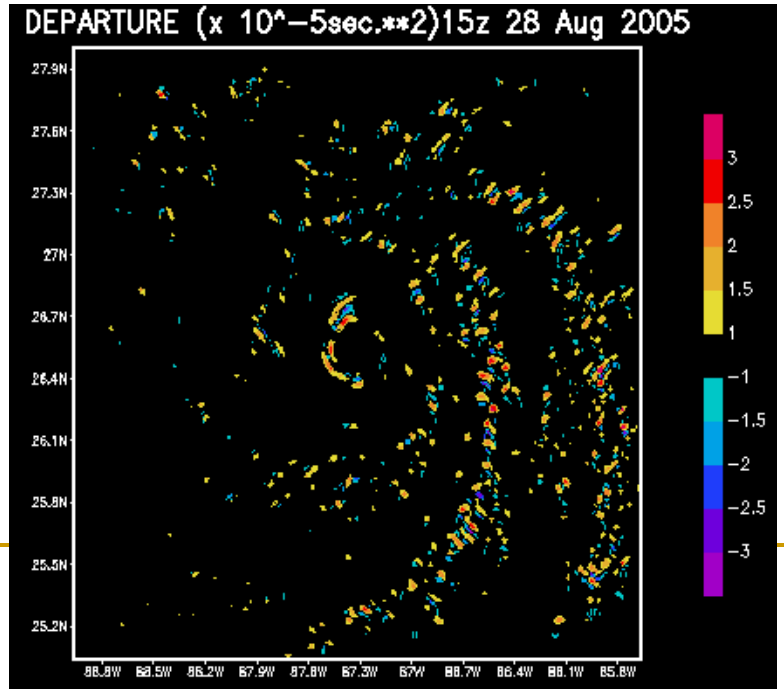

Gradient Wind Departure

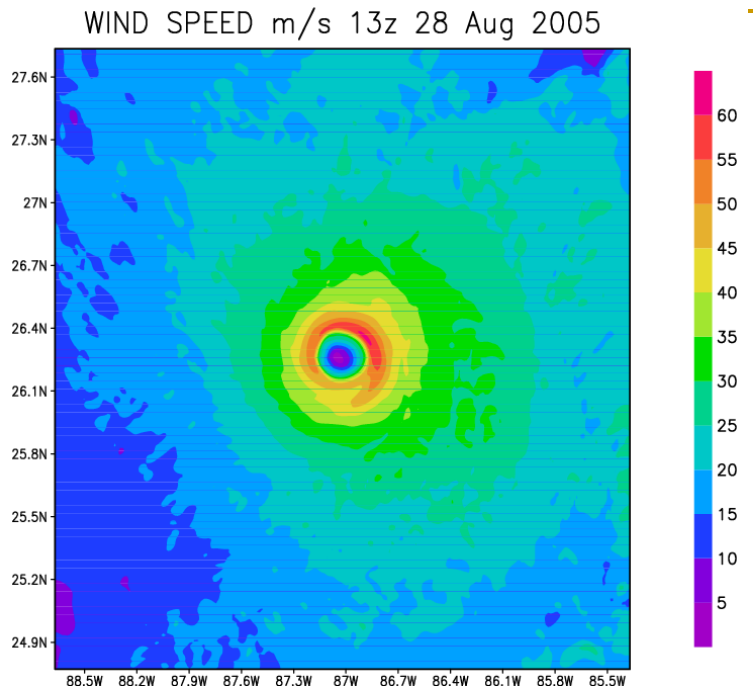
WIND SPEED m/s 13z 28 Aug 2005
27.6N
27.3N
27N
26.7N
26.4N
26.1N
25.8N
25.5N
25.2N
24.9N
88.5W 88.2W 87.9W 87.6W 87.3W 87W 86.7W 86.4W 86.1W 85.8W 85.5W
60
55
50
45
40
35
30
25
20
15
10
5

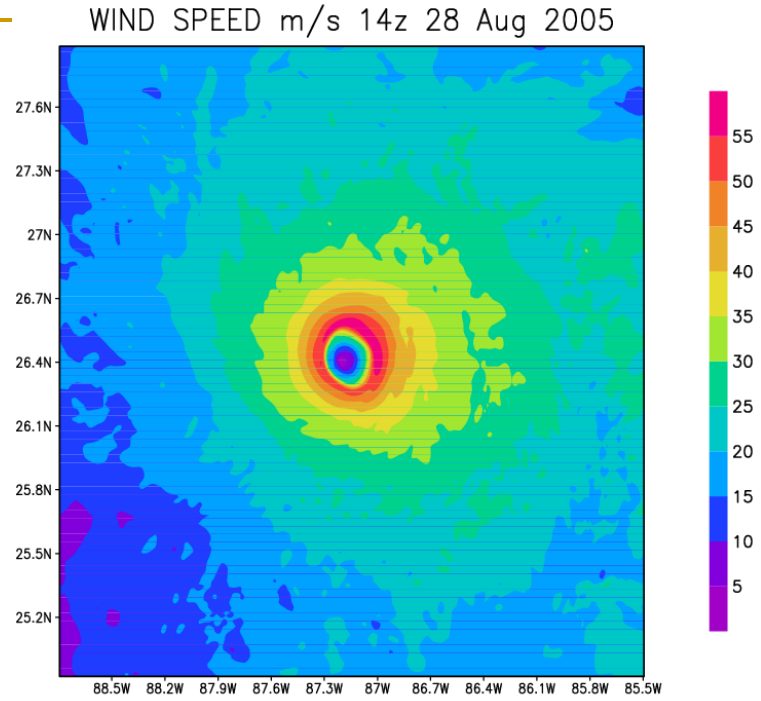
WIND SPEED m/s 14z 28 Aug 2005
27.6N
27.3N
27N
26.7N
26.4N
26.1N
25.8N
25.5N
25.2N
88.5W 88.2W 87.9W 87.6W 87.3W 87W 86.7W 86.4W 86.1W 85.8W 85.5W
55
50
45
40
35
30
25
20
15
10
5

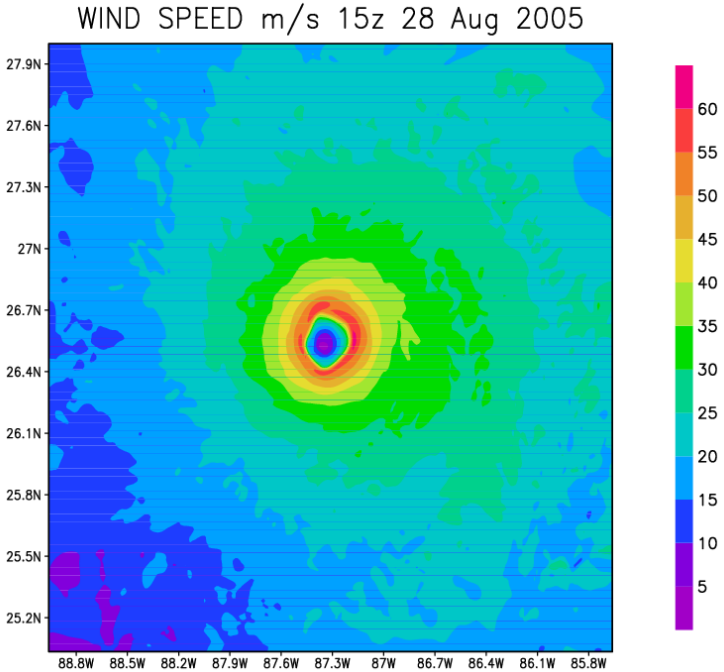
WIND SPEED m/s 15z 28 Aug 2005
27.9N
27.6N
27.3N
27N
26.7N
26.4N
26.1N
25.8N
25.5N
25.2N
88.8W 88.5W 88.2W 87.9W 87.6W 87.3W 87W 86.7W 86.4W 86.1W 85.8W
60
55
50
45
40
35
30
25
20
15
10
5

Life cycle of a cloud

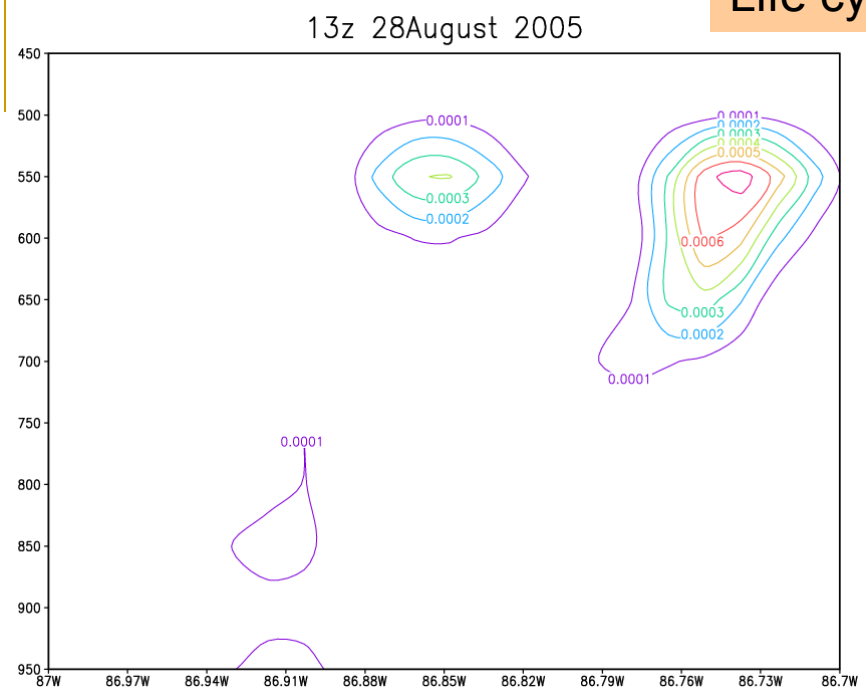

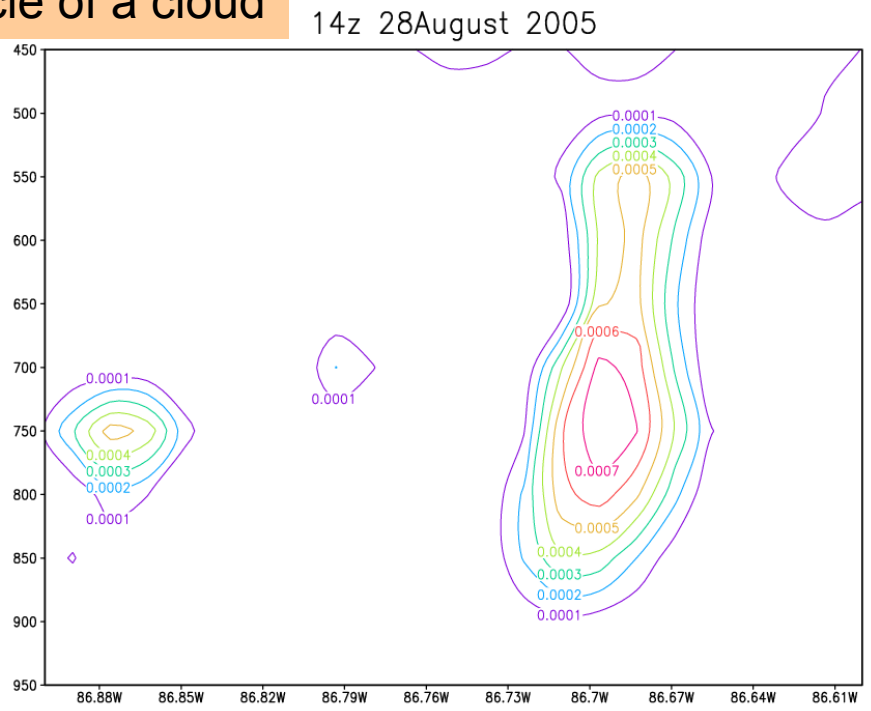

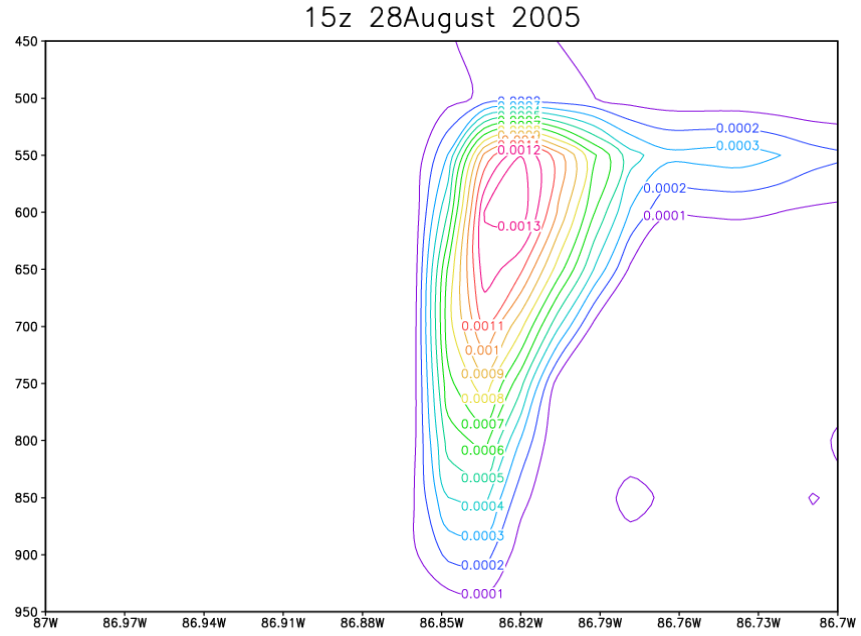

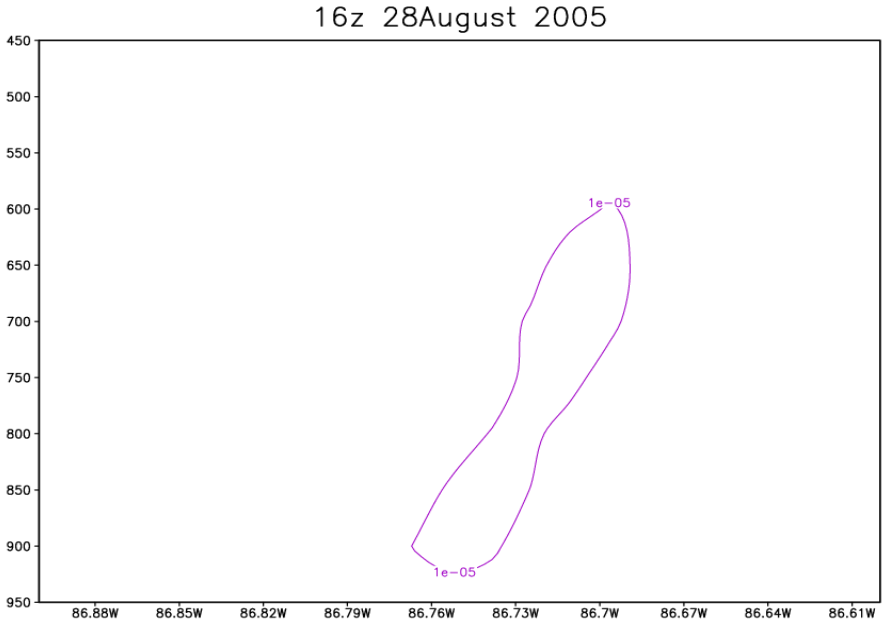

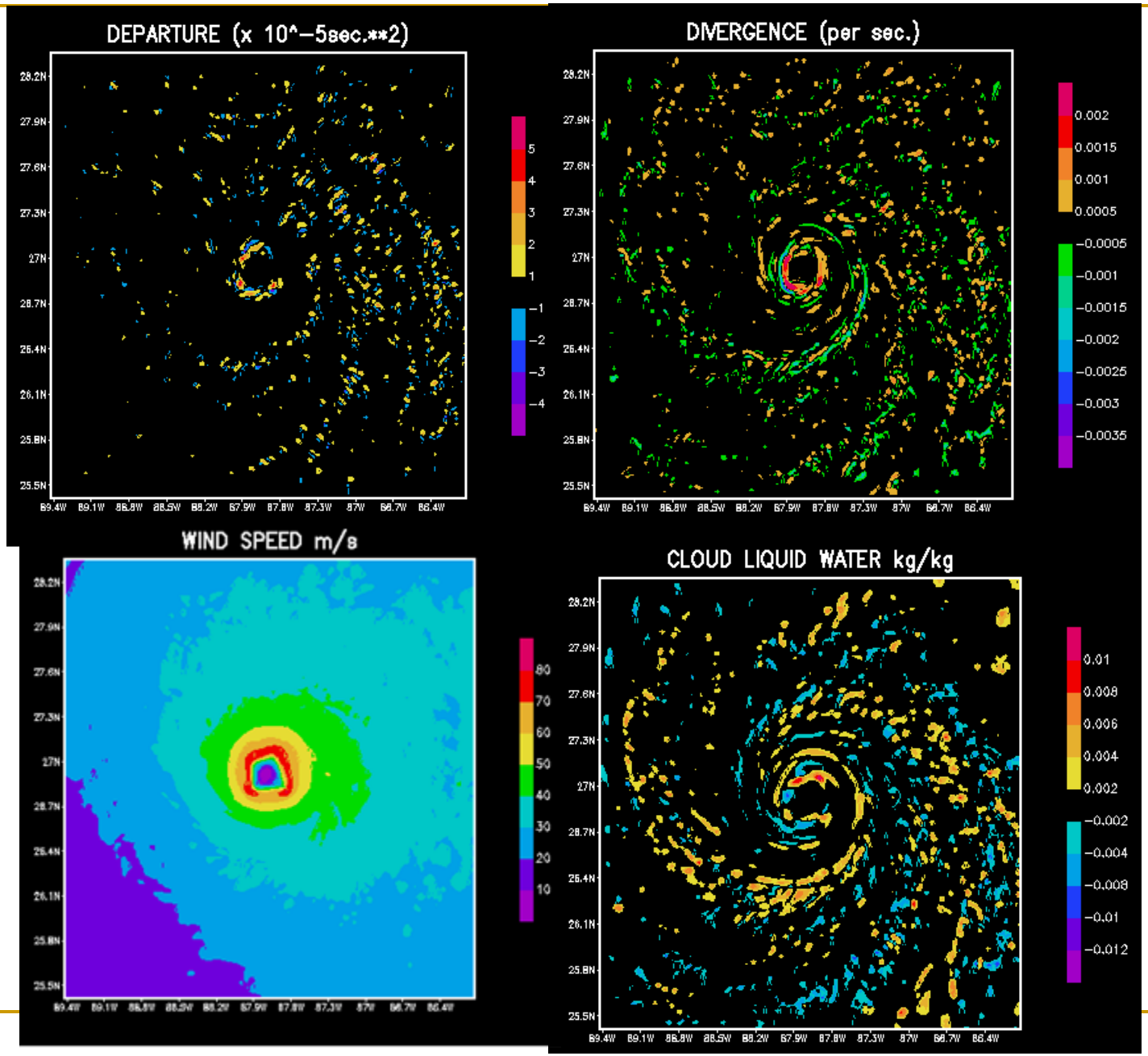

28 August

2005

1600 UTC

NASA GRIP Experiment- FSU Intensity Forecast Enhancement

- The Global Hawk or the ER-2 leave Dryden/Edwards AFB, or the DC-8 flies into the storm
- The plane observes the storm environment from above
- It transmits data to NASA GSFC via a Communications Satellite
- NASA GSFC transmits the data in near real-time to FSU
- FSU interprets the data to forecast imminent Intensity changes
- FSU sends the results to Mission Scientists

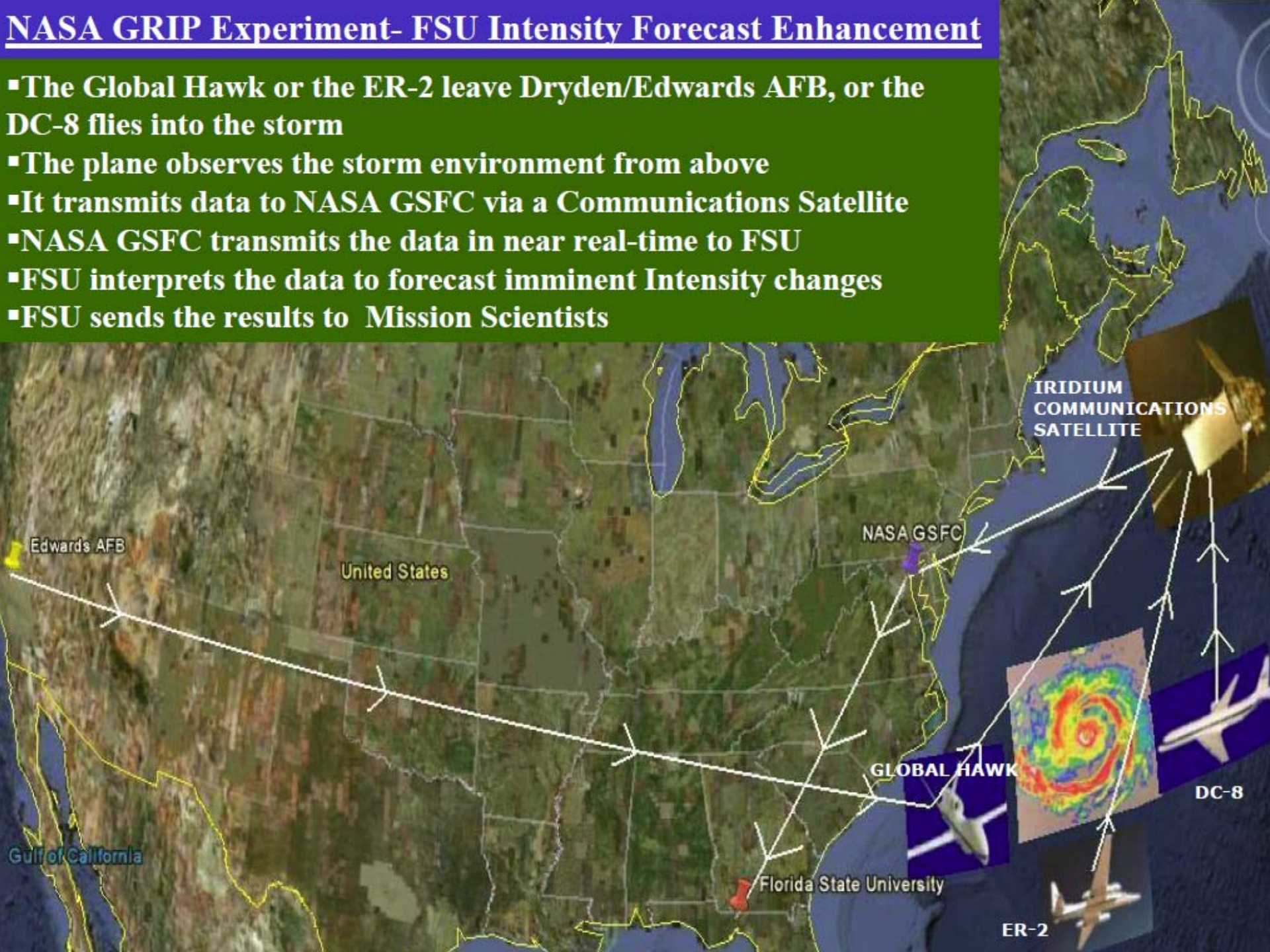

Observations Required

- Radar Reflectivity
- 3-Dimensional Winds
- Pressure Altitude

NASA Dryden Flight Research Center Photo Collection
http://www.dfrc.nasa.gov/Gallery/Photo/index.html
NASA Photo: ED08–0309–24 Date: December 11, 2008 Photo By: Tony Landis

This and a companion Global Hawk unmanned aircraft are used by NASA for Earth science missions and by Northrop Grumman for developmental testing.

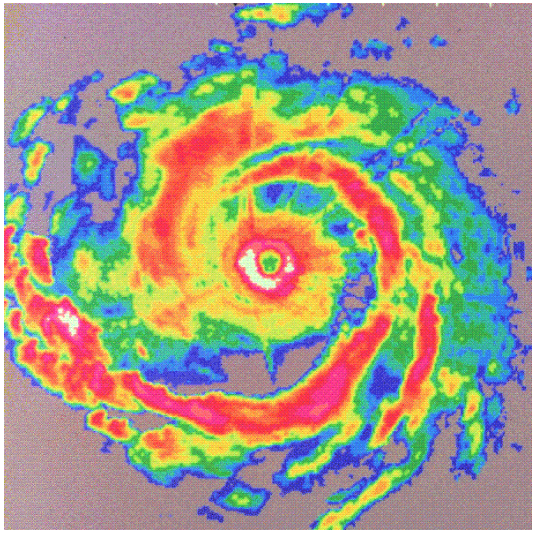

Analyze the field of rain water mixing ratio and compute vertically integrated rain water mixing ratio

Tag cloud bursts

Airborne radar hydrometers

u, v, Φ from airborne radar based (P3s, ER2 and UAVs) and dropwindsonde data

perform an assimilation on real or near-real time for Vθ, Vr and Φ in local cylindrical storm-centered co-ordinates

Calculate the divergence field

Calculate the gradient wind departures

Asses the degree of super gradient wind and calculate the hurricane intensity

Future work

- Future work on mesoscale modeling during the hurricane season of 2009 will include the following models: HWRF(EMC), WRF/ARW (NCAR), COAMPS (NRL),GFDL(NOAA), HWRF-X (HRD), MM5 (FSU), WRF(FSU).

THANKS